Generalised 2D Penrose tilings: structural properties

1987 J. Phys. A: Math. Gen. 20 687

(http://iopscience.iop.org/0305-4470/20/3/031)

J. Phys. A: Math. Gen. 20 (1987) 687-702. Printed in the UK

Generalised 2D Penrose tilings: structural properties

A Pavlovitch† and M Kléman‡

† DTch/SRMP, CEN Saclay, BP 2, 91191 Gif-sur-Yvette, France
‡ Laboratoire de Physique des Solides (associé au CNRS), Université Paris-Sud, Bâtiment 510, 91405 Orsay Cédex, France

Received 21 April 1986

Abstract. Usual Penrose tilings are defined by a set of five phases γ_j which add up to an integer. We study the general case where the phases add up to any number and show that these generalised tilings can be obtained with four tiles (two thick rhombi and two thin rhombi) with different colourings of the edges. The consideration of generalised tilings is relevant for the study of phase distortions, local structural transitions, and therefore various defects of the usual tilings.

1. Introduction

Since the remarkable discovery in 1984 of Al–Mn quenched alloys whose diffraction patterns show up fivefold symmetry (Shechtman *et al* 1984), a number of papers have tried to deepen the structural properties (Audier and Guyot 1986, Bancel *et al* 1985, and many others) of these aperiodic crystals (a term we prefer to quasicrystals). It is now understood that these most peculiar symmetry properties are the 3D images of the very simple symmetries of a cubic lattice in a 6D space, after the manner of the symmetry properties of more usual incommensurate crystals, which can be described in a $(3+n)$-dimensional space, for n degrees of incommensuration (Janner and Janssen 1977). While these degrees of incommensuration bear on the lattice parameters, in aperiodic crystals, the absence of translational symmetries takes root in the non-crystallographic rotational symmetries which are imposed. In both cases the analysis of the projection from the high-dimensional space to real space brings understanding to the structural properties of the non-usual crystallographic phase and to the description of their fundamental modes. Important advances in this direction are the theoretical papers of Mackay (1982), de Bruijn (1981), Kramer and Néri (1984) and Duneau and Katz (1985).

An important problem which relates directly to structural properties is the problem of topological defects; it is known that in usual crystals defects locally break the symmetry group and can be classified by some topological properties of this group (Kléman *et al* 1977). The same happens to be true in aperiodic crystals with some interesting peculiar new features, which were described in Kléman *et al* (1986, hereafter referred to as I) in some detail for the case of 2D aperiodic crystals (which exist in nature, as demonstrated by Bendersky (1985)), whose structure is nothing other than the celebrated Penrose tilings. These tilings were studied in great detail by de Bruijn (1981) using algebraic methods and we relied greatly on this analysis. Most of the results extend to 3D aperiodic crystals.

Dislocations in aperiodic crystals are classified by the first homotopy group of the torus T^6 (3D crystals) or T^4 (2D Penrose tilings); they can also be made through a Volterra process (which reveals the underlying hidden translational symmetries) which has to be followed by rearrangement of the structure. Such rearrangements do not exist in the usual crystals. In aperiodic crystals these rearrangements are essential: they can be analysed in canonical modes of deformation (phasons and structural transitions) which have no equivalent in usual crystals (Lévine *et al* 1985). We have indicated how such transitions occur in Penrose tilings (I) and have shown in particular that the consideration of generalised Penrose tilings permit one to extend the types of dislocations created (introducing imperfect dislocations) and to describe more precisely the rearrangements which occur after the Volterra process. The purpose of this paper is to discuss in depth the structural properties of these generalised tilings, which require the consideration of a 5D space.

This paper is organised as follows. In § 2 we recall de Bruijn's approach to the Penrose tilings. In § 3 we demonstrate that generalised tilings require the introduction of two new tiles with new colouring rules. Generalised tilings depend on an extra free phase γ, which takes continuous values. We study how the tilings evolve when γ varies continuously and how the new tiles arrange in the tiling. Finally we compare some properties of the generalised tilings with those of the usual tiling.

2. De Bruijn's theory of Penrose tilings

In 1981 de Bruijn presented an algebraic theory of Penrose tilings. We recall his results.

Let us consider the arrowed tiles T and t (figure 1(a)) and build with them a tiling of the plane such that the simple (double) arrows match along the common edges, with the same direction. The pattern thus obtained (figure 2) has the following properties.

(i) *Aperiodicity.* There is no translation which leaves the pattern invariant.

(ii) *Indeterminacy of the construction process.* An infinite pattern is not determined by a finite region. Starting from a finite region, there is an (uncountable) infinity of ways to continue the construction.

(iii) *Local isomorphism.* Different infinite patterns are in some sense equivalent, although these are not superposable: any region, however large it might be, belonging to a given infinite tiling, exists in any other different infinite tiling.

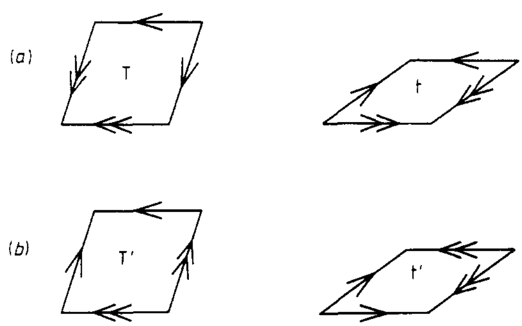

Figure 1. (a) Old tiles. (b) New tiles.

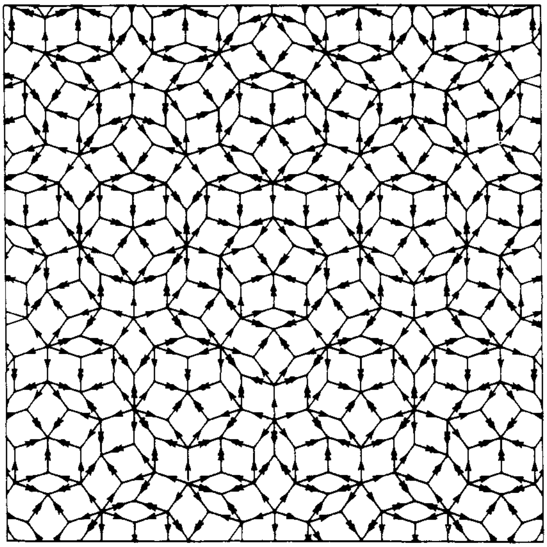

Figure 2. A tiling of the plane using old tiles.

(iv) *Self-similarity.* It is possible to associate to any tiling a different tiling whose tiles are smaller and in the length ratio τ ($\tau = \frac{1}{2}(1+\sqrt{5})$) with the former, and which includes all the vertices of the former tiling.

De Bruijn has demonstrated these properties by using two approaches:

(1) the study of a 5-grid associated with a tiling;

(2) the representation of a tiling as a projection on a 2-plane of the vertices (with integer coordinates) of a simple hypercubic lattice built in a five-dimensional space.

Since our results are extensions of de Bruijn's results and methods, we present these two approaches.

2.1. *Tiling and 5-grid*

An infinite tiling contains strips of adjacent rhombi, with parallel edges. If we join the midpoints of these edges by a curve and repeat this procedure for all the strips of the tiling, we get a grid that is dual from the pattern we started from. In fact de Bruijn shows that this grid could be deformed without topological changes into five bundles of straight lines perpendicular to the pentagonal directions $\boldsymbol{\nu}_i (i = 0, 1, 2, 3, 4)$ with

$$\nu_i = (\cos \tfrac{2}{5} i \pi, \sin \tfrac{2}{5} i \pi).$$

In the following we call this deformed grid a 5-grid. The exact definition is as follows: any point M belonging to the grid obeys the relation

$$\boldsymbol{OM} \cdot \nu_j + \gamma_j = \text{integer} \qquad j = 0, 1, 2, 3, 4. \tag{1}$$

If Z is the complex coordinate of a point M on this grid and if $\zeta = \exp(\frac{2}{5} i \pi)$, this equation also becomes

$$\mathrm{Re}[Z\zeta^{-j}] + \gamma_j = \text{integer} \tag{1'}$$

(we will frequently use this complex notation). The γ_j are real numbers which, in the case studied by de Bruijn, obey the relation

$$\sum_{j=0}^{4} \gamma_j = \text{integer}. \tag{2}$$

It is clear that the tiling (figure 2) and the 5-grid (figure 3) are in a dual relationship.

The use of the 5-grid allows us to demonstrate an important property. Let γ_j be five real numbers obeying relation (2) and let us consider the corresponding 5-grid and its dual lattice. The 'colouring theorem' states that there is only one way to 'colour' the lattice in t and T tiles, i.e. to arrow the edges of this lattice.

2.2. *Tiling and five-dimensional space*

Let us consider a five-dimensional space E_5 and in this space a 2-plane $P(\gamma_j)$ defined by

$$\begin{aligned}
&\sum_{j=0}^{4} (x_j - \gamma_j) = 0 \\
&\sum_{j=0}^{4} \operatorname{Re} \zeta^{2j}(x_j - \gamma_j) = 0 \qquad (3)\\
&\sum_{j=0}^{4} \operatorname{Im} \zeta^{2j}(x_j - \gamma_i) = 0
\end{aligned}$$

with

$$\sum \gamma_j = \text{integer}.$$

This space E_5 is naturally divided into three subspaces P, P′ and D which intersect at the point $\boldsymbol{\gamma}$; $P'(\gamma_j)$ is a 2-plane perpendicular to the two vectors $\operatorname{Re} \zeta^j$ and $\operatorname{Im} \zeta^j$ (i.e. P′ is perpendicular to P) and to the direction D; $D(\gamma_j)$ is directed along (1, 1, 1, 1, 1) (see appendix 1)

$$\mathrm{P} \oplus \mathrm{P}' \oplus \mathrm{D} = \mathrm{E}_5. \tag{4}$$

The *tiling* associated with a set of γ_j obtains by projecting on P the vertices Q of the simple hypercubic lattice of E_5 with integral coordinates which belong to a strip

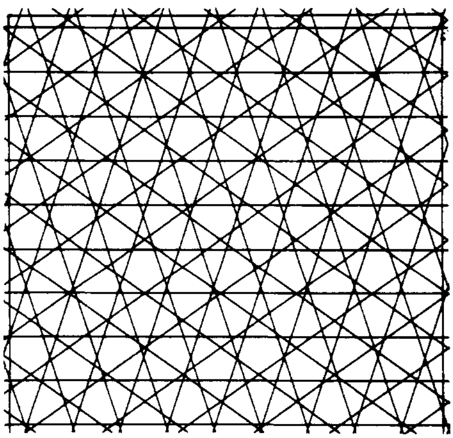

Figure 3. A 5-grid associated with the tiling of figure 2.

of constant thickness, limited by the 2-planes $P(\gamma_j - \frac{1}{10}\sqrt{5})$ and $P(\gamma_j + \frac{1}{10}\sqrt{5})$. This construction was also used by Duneau and Katz (1985) and Kalugin *et al* (1985). We shall also have to consider the projections Y of the vertices Q on the subspace P′⊕D complementary to P in E_5. In particular, the projection of only one of the Q on P′⊕D can inform us on the whole Penrose tiling associated with the strip. We come back to this important question later.

The *5-grid* itself can also be visualised in E_5: it is the intersection with P of the reticular 4-planes of the simple hypercubic lattice perpendicular to the canonic basis. The vectors $\boldsymbol{\nu}_j$ are in P, whose natural basis $(\boldsymbol{a}_1, \boldsymbol{a}_2)$ has components $\{\mathrm{Re}\,\zeta^j\}$ and $\{\mathrm{Im}\,\zeta^j\}$ in E_5 (see appendix 1). This geometrical construction of the 5-grid was extensively used in I for the classification of defects.

3. Generalised tilings

Here we study in detail, in the de Bruijn way, the case where the five real numbers γ_j do not sum to an integer. This investigation yields a non-trivial extension of the 'colouring theorem' and introduces new tiles.

3.1. Extension of the colouring theorem

Let us consider a generalised 5-grid ($\Sigma_{i=0,4}\, \gamma_i \neq$ integer): we prove that the associated tiling can be coloured using t, T and two new tiles t′ and T′ (figure 1(*b*)), with the usual matching rules.

We associate with every mesh of the 5-grid five integers $K_j (j = 0, \ldots, 4)$:

$$K_j\,(\text{mesh}) = K_j\,(Z\text{-mesh}) = \lceil \mathrm{Re}(Z\zeta^{-j}) + \gamma_j \rceil \tag{5}$$

where $\lceil a \rceil$ is the smallest integer larger than a. We note that K_j changes by one unit when we cross a line of the 5-grid perpendicular to the direction $\boldsymbol{\nu}_j$: in the positive sense $K_j \to K_j + 1$; in the negative sense $K_j \to K_j - 1$.

The K_j are constant for a given mesh. In order to distinguish between the points of coordinates Z of a given mesh we introduce five real numbers λ_j $(j = 0, \ldots, 4)$:

$$\lambda_j(Z) = K_j(Z) - (\mathrm{Re}(Z \cdot \zeta^{-j}) + \gamma_j). \tag{6}$$

It is clear that

$$0 < \lambda_j < 1 \qquad (j = 0, 4).$$

When the 5-grid is regular (no more than two lines crossing at one point), only two λ_j can be equal to zero for a given Z. We have

$$\sum_{j=0}^{4} \lambda_j(Z) = \sum_{j=0}^{4} K_j(Z) - \left(\sum_{j=0}^{4} \mathrm{Re}(Z \cdot \zeta^{-j}) + \sum_{j=0}^{4} \gamma_j \right) \tag{7}$$

which yields

$$\sum_{j=0}^{4} \lambda_j(Z) = \sum K_j(Z) - \sum \gamma_j \tag{8}$$

when

$$\gamma = \sum \gamma_j = \text{integer}$$

$$\gamma < \sum K_j(Z) < \gamma + 5$$

so that $\Sigma\, K_j(Z)$ takes only four values:

$$\gamma+1, \quad \gamma+2, \quad \gamma+3, \quad \gamma+4. \tag{9}$$

Otherwise, it takes five values

$$\lceil\gamma\rceil, \quad \lceil\gamma\rceil+1, \quad \lceil\gamma\rceil+2, \quad \lceil\gamma\rceil+3, \quad \lceil\gamma\rceil+4. \tag{10}$$

Consider now the tiling associated with the 5-grid. It is made of points with coordinates:

$$Z = \sum_{j=0}^{4} (K_j - \gamma_j)\zeta^j$$

where each vector $\boldsymbol{K}$ corresponds to a mesh in the 5-grid. We call the 'index of a vertex' the quantity

$$K = \sum_{j=0}^{4} K_j. \tag{11}$$

The colouring rules are obtained in two steps: we first define the double arrows; then a lemma will lead to the distribution of the simple arrows.

Let us begin with a simple remark; consider a line of the bundle F_0 perpendicular to $\boldsymbol{\nu}_0$, and let us index the meshes situated to its left. We find that $K \to K+1$ when we cross a line belonging to the bundles F_1 or F_2 and that intersections with the lines of bundles F_1 and F_4 alternate (the same holds for F_2 and F_3). The index at the left of the considered line can take only three values.

Because in the 5-grid the index takes in general five values, there are therefore two types of line: the lines of type 1 at the left of which the index takes the values $\lceil\gamma\rceil$, $\lceil\gamma\rceil+1$, $\lceil\gamma\rceil+2$ and the line of type 2 where the index is equal to $\lceil\gamma\rceil+1$, $\lceil\gamma\rceil+2$, $\lceil\gamma\rceil+3$.

Let us now introduce the double arrows, using de Bruijn's method: for lines of type 1 we put double arrows on edges which are crossing this line from vertex with index $\lceil\gamma\rceil+1$ to vertex with index $\lceil\gamma\rceil$ and from vertex with index $\lceil\gamma\rceil+2$ to vertex with index $\lceil\gamma\rceil+3$. For lines of type 2, the result is analogous: the double arrows go from $\lceil\gamma\rceil+2$ to $\lceil\gamma\rceil+1$ and from $\lceil\gamma\rceil+3$ to $\lceil\gamma\rceil+4$.

Finally, we put simple arrows on all the other edges of the tiling and direct them towards the vertex which contains the obtuse angle of the tiles incident to the considered edge; this is done in an unique way, since according to the lemma proved in appendix 2 (and which generalises de Bruijn's lemma), the new tiles T′ and t′ (figure 1(b)) as well as the old tiles always join with their obtuse angles at the same vertex.

We note here an important feature: the new tiles T′ and t′ are always at the intersection of two lines of different types, while the old tiles T and t are at the intersection of two lines of the same type (figure 4). Figures 5(a) and (b) show some tilings of the plane with $\gamma \neq$ integer. We note that the tilings get naturally divided into islands made of old tiles (which could eventually be continued to infinity), separated by walls of new tiles arranged along lines of the second type. The diameter of those islands scales like $1/\gamma$. This is most visible in figure 6, which is a tiling extended to 3000 tiles.

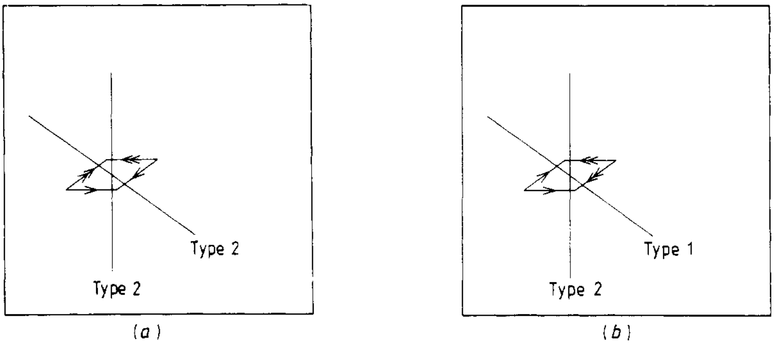

Figure 4. (*a*) Old tile at the intersection of two lines of the 5-grid of the same type. (*b*) New tile at the intersection of two lines of the 5-grid of different types.

3.2. *Five-dimensional representation*

As already noticed by Duneau and Katz (1985), whatever the value of $\Sigma\ \gamma_i$ might be, the projection V on the complementary of P in E_5 of the points that projects on the tiling is included inside the projection on this subspace of the hypercube strip centred on the point of coordinates $\boldsymbol{\gamma}$ which is a rhombic icosahedron I (figure 8(*a*)). The projection V, for γ = integer, is obtained as the cut of I by four 2-planes $P'(K_j)$ (parallel to the plane $P'(\gamma_j)$ defined above), with $\Sigma\ K_j = K$ taking one of the four values $\gamma+1$, $\gamma+2$, $\gamma+3$, $\gamma+4$, passing through the point $\boldsymbol{K} = (K_0, \ldots, K_4)$ of the 5D space. Each subset consists of a pentagon V_i; for example V_1 (for $K = 1$) has vertices with complex coordinates 1, ζ, ζ^2, ζ^3, ζ^4, in this plane, and any point $Y = \Sigma\ \lambda_j \zeta^{2j}$ in V_1 corresponds to a vertex of index $\Sigma\ K_j = 1$, whose coordinate in P is $\Sigma\ (K_j - \gamma_j)\zeta^j$. De Bruijn shows that the nature of the vertex (i.e. to which of the eight types of vertices shown in figure 7 it belongs) is entirely defined by the location of Y in V_1 (figure 8(*b*)) which is partitioned into polygonal subregions corresponding respectively to vertices S, K and Q. The V_i are densely filled by the projection of points of the hypercubic lattice.

Consider indeed a vertex of type Q in the case $\Sigma\ \gamma_i$ = integer. Such a vertex only appears when its index is equal to $\gamma+1$ or $\gamma+4$. Its projections on $P(K_j)$ and $P'(K_j)$ are:

$$Z = \sum_{j=0,4} (K_j - \gamma_j)\zeta^j \qquad \text{and} \qquad Y = \sum_{j=0,4} (K_j - \gamma_j)\zeta^{2j}. \tag{12}$$

In real notation:

$$Z = \sum_{j=0,4} (K_j - \gamma_j)\boldsymbol{\zeta}^j \qquad \text{and} \qquad Y = \sum_{j=0,4} (K_j - \gamma_j)\boldsymbol{\mu}_j$$

where $\boldsymbol{\nu}_j = (\cos \frac{2}{5}\pi i, \sin \frac{2}{5}\pi i$ and $\boldsymbol{\mu}_j = (\cos \frac{4}{5}\pi i, \sin \frac{4}{5}\pi i)$. (Figures 9(*a*) and 9(*b*)). In figure 9(*c*) we have redrawn V_1 (assuming that $K = \gamma + 1$) and drawn V_2 which contain the projections of the neighbours of Q in P, since their index is $\gamma+2$. The hatched region represented in figure 9(*c*) has the following meaning: if a vertex of the tiling projects on it we can say that it will be a Q type vertex.

All these considerations generalise to the case where $\Sigma_{i=0,4}\ \gamma_i \neq$ integer. We then get the partition of figure 10(*a*)-(*e*); there are now five subsets V_i corresponding to the five values of the index $\lceil\gamma\rceil \ldots \lceil\gamma\rceil+4$, each of them divided into regions corresponding to some vertex of a generalised pattern. There are now 28 new vertices, drawn in figure 11. Five of them have a hand; hence if we add their chiral image, there are in fact 33 new vertices.

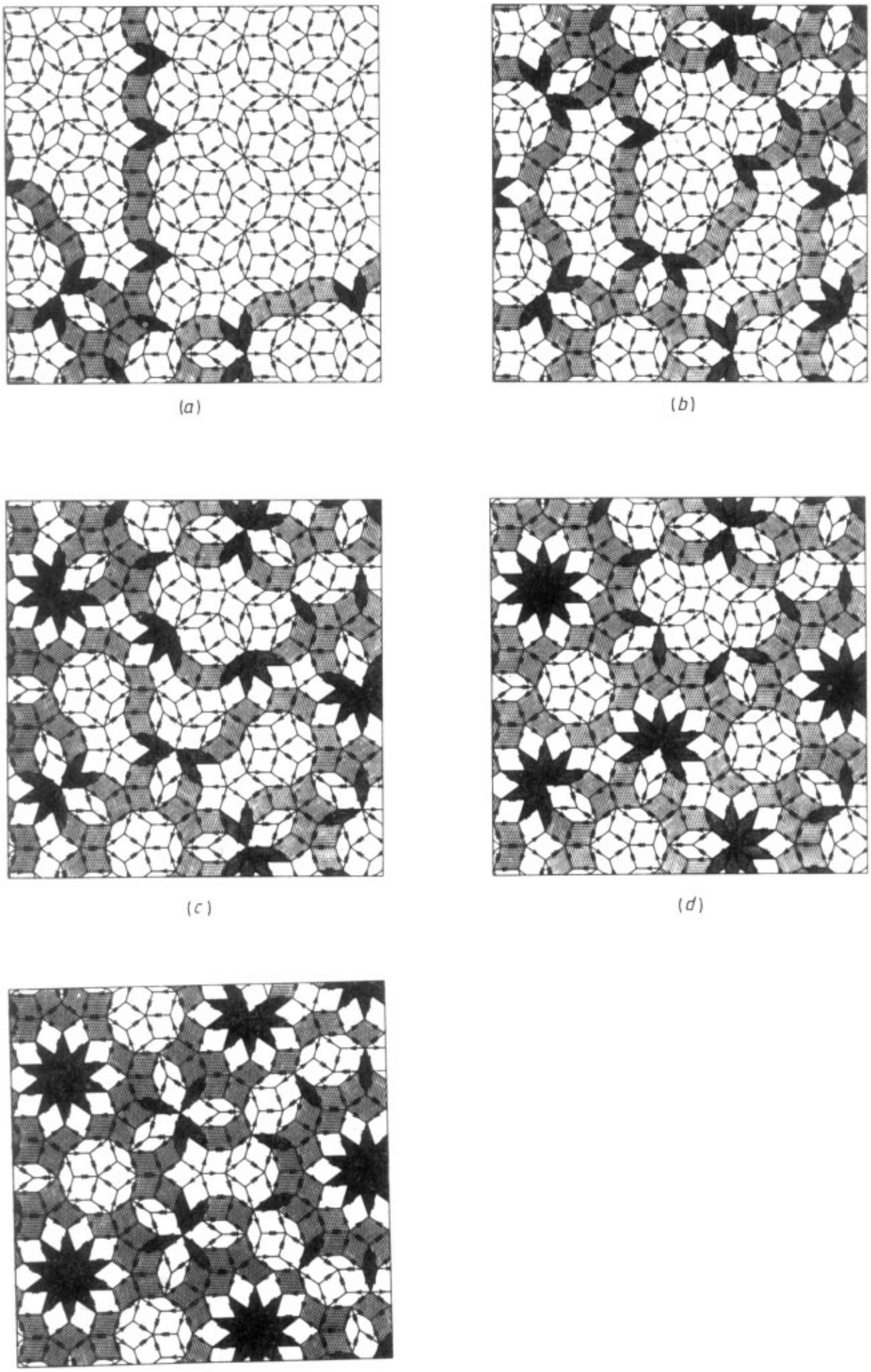

Figure 5. Generalised tilings for (*a*) $\Sigma\gamma_j = 0.1$, (*b*) $\Sigma\gamma_j = 0.2$, (*c*) $\Sigma\gamma_j = 0.3$, (*d*) $\Sigma\gamma_j = 0.4$, (*e*) $\Sigma\gamma_j = 0.5$. 500 tiles approximately are in each tiling; the new tiles are shaded.

Figure 6. Generalised tiling for $\Sigma\gamma_j = 0.1$ with approximately 3000 tiles. Note the division in islands of old tiles.

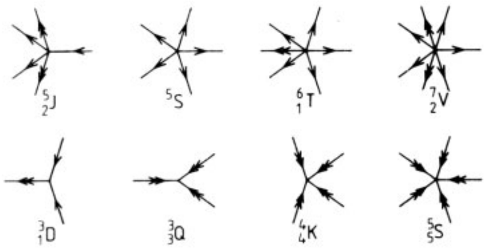

Figure 7. Old vertices: the capital letter indicates the topology of the vertex (defined by the succession of angles between bonds), the upper index is the number of bonds and the lower one the number of double arrows. we have kept as much as possible de Bruijn's notation for the capital letter.

3.3. Densities of tiles

Let us research how the lines of a given type (1 or 2) are located in a bundle F_i, along the direction $\boldsymbol{\nu}_i$. It is easy to prove that the quantity

$$t_i = \lceil \gamma + K_i/\tau \rceil + \lceil -K_i/\tau \rceil \tag{13}$$

takes the values $t_i = 1$ on a line of type 1 and $t_i = 2$ on a line of type 2; K_i is an integer which increases by one unit from one line to the next one along $\boldsymbol{\nu}_i$. One can see that the lines $t_i = 2$ are located quasiperiodically, with three periods which are three consecutive numbers of the Fibonacci sequence. More precisely, when $\tau^k < 1/\gamma < \tau^{k+1}$ the periods are f_k, f_{k+1}, f_{k+2}, where

$$f_k = \frac{1}{\tau+2}[\tau^{k+2} + (-\tau)^{-k}].$$

When $1/\gamma = \tau^k$, there are only two periods f_k and f_{k+1}.

The densities of new tiles vary quadratically with γ. We have explicitly

$$t = (2-\tau)[2\gamma^2 - 2\gamma + 1] \qquad t' = 2(2-\tau)[-\gamma^2 + \gamma]$$

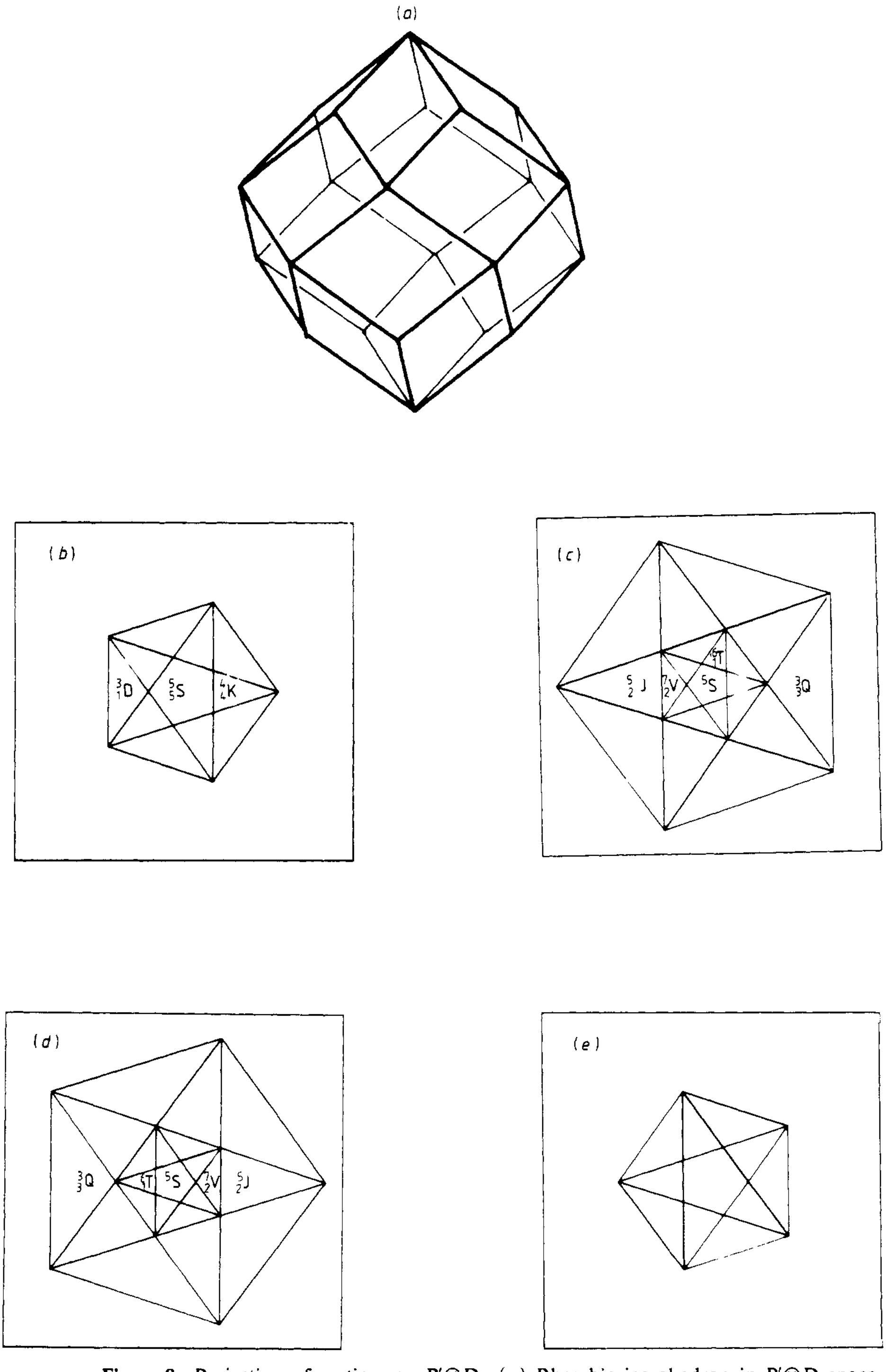

Figure 8. Projection of vertices on P′⊗D. (*a*) Rhombic icosahedron in P′⊗D space, centred on $\boldsymbol{\gamma}$, (*b*) V_1: index $K = \gamma + 1$, (*c*) V_2: index $K = \gamma + 2$, (*d*) V_3: index $K = \gamma + 3$, (*e*) V_4: index $K = \gamma + 4$.

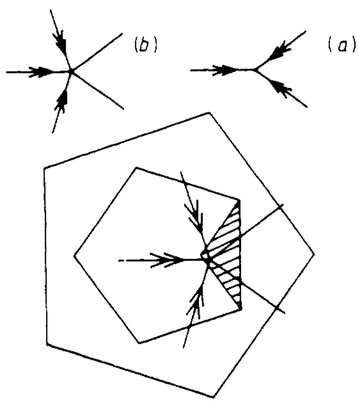

Figure 9. (a) Vertex Q projected on P from some vertex of the hypercube, with bonds joining it to its neighbours, all belonging to the strip. (b) Projection of the same set in P': the vertex itself belongs to P'($\gamma+1$), while the vertices at the end of the bonds belong to P'($\gamma+2$). (c) V_1 with vertices $1, \zeta, \zeta^2, \zeta^3, \zeta^4$ and V_2 with vertices $1+\zeta, 1+\zeta^2, \zeta^2+\zeta^3, \zeta^3+\zeta^4, \zeta^4+1$. If the considered Q belongs to V_1, its neighbours are in V_2. The shaded area represents the projection of a $^3_3$Q type vertex. In fact, if one crossses the right boundary of the shaded area, one gets a $^4_4$K vertex.

$$T=(\tau-1)[2\gamma^2-2\gamma+1] \qquad T'=2(\tau-1)[-\gamma^2+\gamma]$$

with $t+t'+T+T'=1$.

A more detailed account of these properties will be given elsewhere.

4. Discussion and conclusion

The properties of the tiling for $\gamma \neq$ integer are worth comparing to those for $\gamma=$ integer, recalled in the introduction.

(i) *Aperiodicity.* This property holds whatever γ might be; the demonstration is as in de Bruijn for $\gamma=$ integer, *mutatis mutandis*, and will not be repeated here.

(ii) *Indeterminacy of the construction process.* Suppose we have constructed an arbitrarily large but finite region R in a tiling defined by a set of γ_i. Call G the corresponding region in a 5-grid; G is not unique. Let d be the smallest distance between a point of intersection in G and the straight lines of bundle F_0. Then the transformation

$$\gamma_0'=\gamma_0+d/2 \qquad \text{and} \qquad \gamma_i'=\gamma_i$$

leaves R unaltered but modifies globally the tiling (with or without introduction of tiles). In practice, any region R can be extended in infinitely many ways to an infinite tiling, with γ_i varying in certain ranges fixed as above.

(iii) *Local isomorphism.* This property also extends for $\gamma \neq$ integer: any region R belonging to a given γ tiling exists in any tiling with the same γ but different γ_i. The demonstration requires the consideration of the projection of R in the V and goes along the same lines as for $\gamma=0$ (de Bruijn).

(iv) *Self-similarity.* As soon as $\gamma \neq$ integer, the associated pattern does not possess *stricto sensu* inflated nor deflated patterns. For instance, in the case of the deflation,

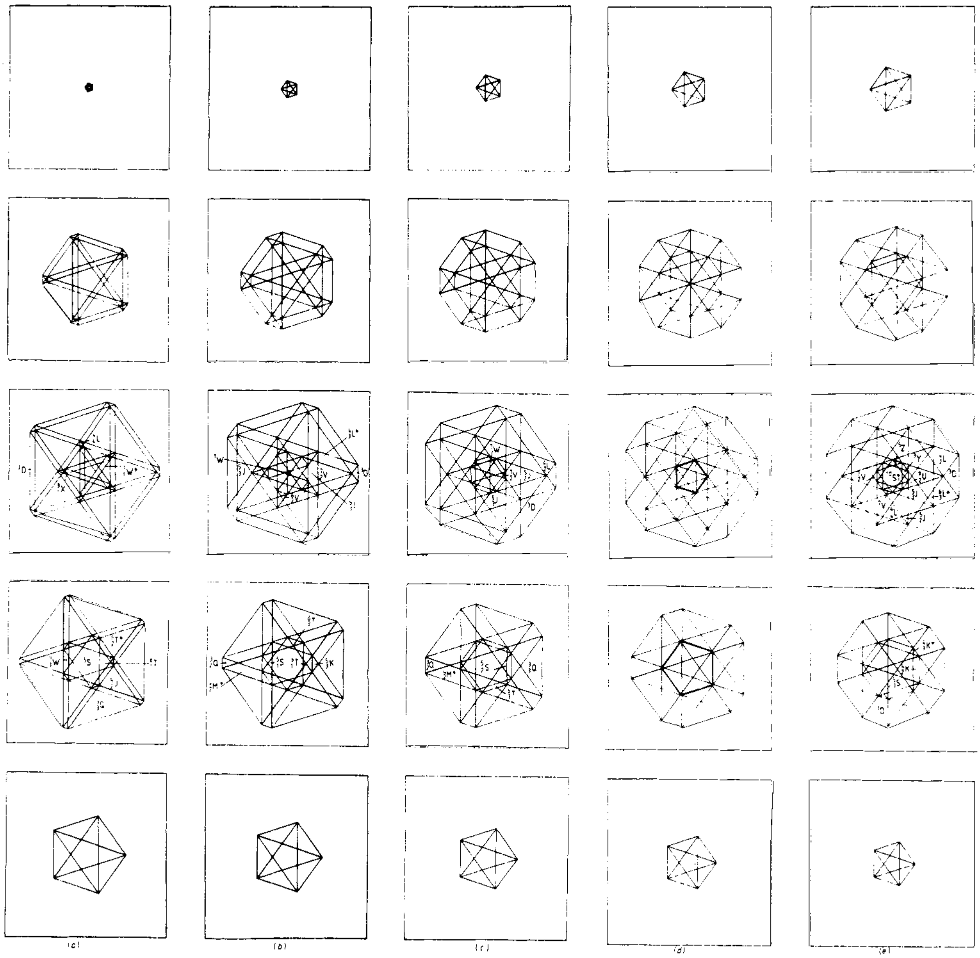

Figure 10. Partition of P′ in V_i for $\gamma \neq$ integer. (*a*) $\gamma=0.1$, (*b*) $\gamma=0.2$, (*c*) $\gamma=0.3$, (*d*) $\gamma=0.4$, (*e*) $\gamma=0.5$. Corresponding vertices are indicated in some domains.

the associated pattern with tiles τ times smaller (obtained by an extension of de Bruijn's method) will not contain all the vertices of the former pattern. The reader is referred to Katz and Duneau (1986) for a demonstration of this property. De Bruijn's rule states that the γ_j' of the deflated tiling are

$$\gamma_j' = \gamma_{j+1} + \gamma_j + \gamma_{j-1}$$

i.e.

$$\gamma' = 3\gamma.$$

Acknowledgments

We wish to thank Professor V Gefen and Professor J Peyrière for discussions. One of us (AP) is greatly indebted to Drs M Guillopé and O Mathieu for useful comments.

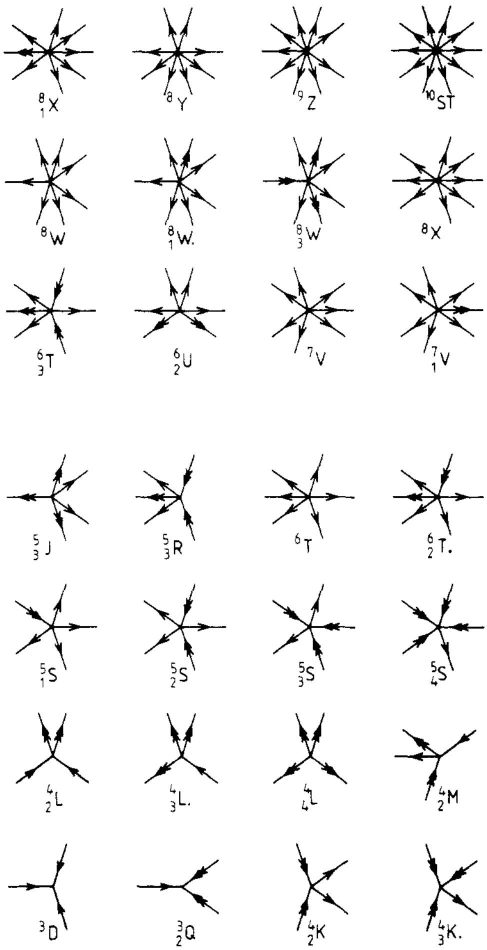

Figure 11. New vertices. Those whose capital letter have dots lack a mirror plane; their enantiomer is therefore also allowed.

Appendix 1

Let $(\boldsymbol{l}_0, \ldots, \boldsymbol{l}_4)$ be the canonical basis of IR^5, and consider the new basis:

$$\boldsymbol{u}_0 = \frac{1}{\sqrt{5}}(1, 1, 1, 1, 1)$$

$$\boldsymbol{u}_1 = \frac{\sqrt{2}}{\sqrt{5}}(\mathrm{Re}\ \zeta^j)_{j=0,4}$$

$$\boldsymbol{u}_2 = \frac{\sqrt{2}}{\sqrt{5}}(\mathrm{Im}\ \zeta^j)_{j=0,4}$$

$$\boldsymbol{u}_3 = \frac{\sqrt{2}}{\sqrt{5}}(\mathrm{Re}\ \zeta^{2j})_{j=0,4}$$

$$\boldsymbol{u}_4 = \frac{\sqrt{2}}{\sqrt{5}}(\mathrm{Im}\ \zeta^{2j})_{j=0,4}.$$

This is an orthonormal basis. The transfer matrix from $(\boldsymbol{l}_i)_{i=0,4}$ to $(\boldsymbol{u}_i)_{i=0,4}$ can be written as

$$\frac{\sqrt{2}}{\sqrt{5}}\begin{pmatrix} 1/\sqrt{2} & 1/\sqrt{2} & 1/\sqrt{2} & 1/\sqrt{2} & 1/\sqrt{2} \\ 1 & \cos\frac{2}{5}\pi & \cos\frac{4}{5}\pi & \cos\frac{6}{5}\pi & \cos\frac{8}{5}\pi \\ 0 & \sin\frac{2}{5}\pi & \sin\frac{4}{5}\pi & \sin\frac{6}{5}\pi & \sin\frac{8}{5}\pi \\ 1 & \cos\frac{4}{5}\pi & \cos\frac{8}{5}\pi & \cos\frac{2}{5}\pi & \cos\frac{6}{5}\pi \\ 0 & \sin\frac{4}{5}\pi & \sin\frac{8}{5}\pi & \sin\frac{2}{5}\pi & \sin\frac{6}{5}\pi \end{pmatrix}.$$

The spaces spanned by $\boldsymbol{u}_0$, $(\boldsymbol{u}_1, \boldsymbol{u}_2)\oplus(\boldsymbol{u}_3, \boldsymbol{u}_4)$ are globally invariant under fivefold rotation about the $\boldsymbol{u}_0$ direction.

Any vector $\boldsymbol{a}$ of coordinates $(\alpha_0, \ldots, \alpha_4)$ in $(\boldsymbol{l}_i)_{i=0,4}$ is projected along $\boldsymbol{\alpha}_p$ in P spanned by $(\boldsymbol{u}_1, \boldsymbol{u}_2)$ as follows:

$$\boldsymbol{a}_p = \frac{\sqrt{2}}{\sqrt{5}}\left[\left(\sum_{i=0,4} \alpha_i \cos\tfrac{2}{5}i\pi\right)\boldsymbol{u}_1 + \left(\sum_{i=0,4} \alpha_i \sin\tfrac{2}{5}i\pi\right)\boldsymbol{u}_2\right].$$

If one identifies $\boldsymbol{u}_1$ and $\boldsymbol{u}_2$ as the real and the complex axes of the complex plane, $\boldsymbol{a}_p$ is

$$a_p = \frac{\sqrt{2}}{\sqrt{5}}\left(\sum_{i=0,4} \alpha_i \zeta^i\right) \qquad \text{or} \qquad \boldsymbol{a}_p = \frac{\sqrt{2}}{\sqrt{5}}\left(\sum_{j=0,4} \alpha_j \boldsymbol{\nu}_j\right).$$

In the case where we restrict to the hypercube $P(0)$:

$$\sum_{j=0,4} \alpha_i = 0.$$

We have the inverse relation

$$\alpha_i = \mathrm{Re}(a_p \zeta^{-j}).$$

The same kind of relation holds for P′ spanned by $(\boldsymbol{u}_3, \boldsymbol{u}_4)$

$$\boldsymbol{a}_{p'} = \frac{\sqrt{2}}{\sqrt{5}}\left[\left(\sum_{i=0,4} \alpha_i \cos\tfrac{4}{5}i\pi\right)\boldsymbol{u}_3 + \left(\sum_{j=0,4} \alpha_i \sin\tfrac{4}{5}i\pi\right)\boldsymbol{u}_4\right]$$

which gives

$$a_{p'} = \frac{\sqrt{2}}{\sqrt{5}}\sum_{j=0,4} \alpha_j \zeta^{2j} \qquad \text{or} \qquad \boldsymbol{a}_{p'} = \frac{\sqrt{2}}{\sqrt{5}}\sum_{j=0,4} \alpha_i \boldsymbol{\mu}_j$$

where

$$\boldsymbol{\nu}_i(\cos\tfrac{2}{5}i\pi, \sin\tfrac{2}{5}i\pi) \qquad \text{and} \qquad \boldsymbol{\mu}_i(\cos\tfrac{4}{5}i\pi, \sin\tfrac{4}{5}i\pi).$$

$\boldsymbol{\nu}_i$ (respectively $\boldsymbol{\mu}_i$) is the normalised projection of $\boldsymbol{l}_i$ on P (respectively P′).

Appendix 2

The aim of this appendix is to prove that the rule that introduces simple arrows does not lead to any inconsistency. Let us restrict to a line of the bundle F_0 perpendicular to $\boldsymbol{\nu}_0$. Assume that this is a line of type 1. We will prove that the arrow which crosses this line is simple only and only if it is situated between intersections with lines of bundles F_p and F_q with $p+q$ odd.

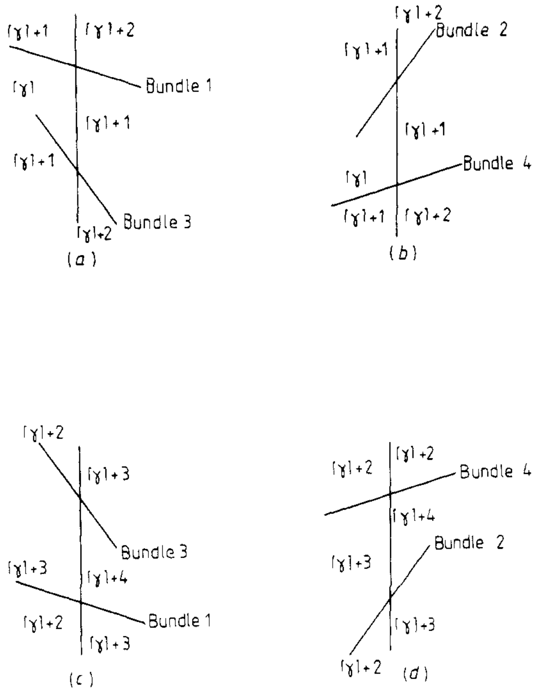

Figure A1.

Consider $(p+q)$ even. All the possible situations are those of figure A1(a)-(d) which shows that the considered arrow is double. Consider for example figure A1(a); the index on the left below the F_2 line and above the F_4 line can be only $\lceil\gamma\rceil$ (the index takes only three values $\lceil\gamma\rceil$, $\lceil\gamma\rceil+1$ and $\lceil\gamma\rceil+2$).

Appendix 3

In this appendix, we describe the projection on $\mathrm{P}'\otimes\mathrm{D}$ of points of Z_5 which project on the tiling in P.

Consider a subject of $IR\times C$:

$$V=\left\{\left(\sum_{j=0,4}\lambda_j,\sum\lambda_j\zeta^{2j}\right),0<\lambda_j<1\right\}.$$

Let (K_0, K_4) be a point of Z_5.

We show that $(K_j)_{j=0,4}$ projects on a point of the tiling associated with $(\gamma_j)_{j=0,4}$ if and only if

$$\left(\sum_{j=0,4}(K_j-\gamma_j),\sum_{j=0,4}(K_j-\gamma_j)\zeta^{2j}\right)\in V. \qquad \text{(A3.1)}$$

Suppose $(K_j)_{j=0,4}$ projects on a point of the tiling in P. Then there is Z with

$$K_j=k_j(Z)=\lceil\mathrm{Re}(Z\zeta^{-j})+\gamma_j\rceil.$$

Let

$$\lambda_j = +K_j(Z) - \mathrm{Re}(Z\zeta^{-j}) + \gamma_j$$

then

$$\sum \lambda_j = \sum (K_j - \gamma_j)$$

and

$$\sum \lambda_j \zeta^{2j} = \sum (K_j - \gamma_j)\zeta^{2j}.$$

Hence (A3.1) is true.

Suppose now that (A3.1) is verified. Then there is $(\lambda_j)_{j=0,4}$ such that

$$\sum \lambda_j = \sum (K_j - \gamma_j)$$

and

$$\sum \lambda_j \zeta^{2j} = \sum (K_j - \gamma_i)\zeta^{2j}$$

which means that the vector $(K_j - \lambda_j - \gamma_j) \in P(0)$.

From appendix 1, there is a Z such that

$$K_j - \lambda_j - \gamma_j = \mathrm{Re}(Z\zeta^{-j})$$

which shows that (K_j) belongs to the tiling.

References

Audier M and Giyot P 1986 *Phil. Mag. Lett.* **53** L43–51
Bancel P A, Heiney P A, Stephens P W, Goldman A I and Horn P M 1985 *Phys. Rev. Lett.* **54** 2422–5
Bendersky L 1985 *Phys. Rev. Lett.* **55** 1461
de Bruijn N G 1981 *K. Nederl. Akad. Wetensch. Proc.* A **84** 51
Duneau M and Katz A 1985 *Phys. Rev. Lett.* **54** 2688
Janner A and Janssen T 1977 *Phys. Rev.* B **15** 643–58
Kalugin P A, Kitaev A Y and Levitov L S 1985 *JEPT Lett.* **41** 145–9
Katz A and Duneau M 1986 *J. Physique* **47** 191–6
Kléman M, Gefen Y and Pavlovitch A 1986 *Europhys. Lett.* **1** 61
Kléman M, Michel L and Toulouse G 1977 *J. Physique* **38** L195–6
Kramer P and Néri R 1984 *Acta Crystallogr.* A **40** 580
Lévine D, Lubensky T C, Ostlund S, Ramaswamy S, Steinhardt P J and Toner J 1985 *Phys. Rev. Lett.* **54** 1424–8
Mackay A L 1982 *Physica* A **114** 609
Shechtman D, Blech I, Gratias D and Cahn J W 1984 *Phys. Rev. Lett.* **53** 1951–3